

Supporting information

Changes in light absorption and molecular composition of water-soluble humic-like substances during a winter haze bloom-decay process in Guangzhou, China

Chunlin Zou^{1,3}, Tao Cao^{1,3}, Meiju Li^{1,3}, Jianzhong Song^{1,2,4,*}, Bin Jiang^{1,2}, WangluJia^{1,2}, Jun Li^{1,2}, Xiang Ding^{1,2}, Zhiqiang Yu^{1,2,4}, Gan Zhang^{1,2}, Ping'an Peng^{1,2,3,4}

¹State Key Laboratory of Organic Geochemistry and Guangdong Provincial Key Laboratory of Environmental Protection and Resources Utilization, Guangzhou Institute of Geochemistry, Chinese Academy of Sciences, Guangzhou 510640, China

²CAS Center for Excellence in Deep Earth Science, Guangzhou 510640, China

³University of Chinese Academy of Sciences, Beijing 100049, China

⁴Guangdong-Hong Kong-Macao Joint Laboratory for Environmental Pollution and Control, Guangzhou 510640, China

*Correspondence to: Jianzhong Song (songjzh@gig.ac.cn)

Contents:

Text S1. Light absorption

Text S2. FT-ICR MS analysis

Text S3. Chemical analysis

Table S1. Meteorological parameters and concentrations of carbon fraction and major ion in PM_{2.5} samples.

Table S2. Average values of Abs₃₆₅, MAE₃₆₅, and AAE of WSOC and HULIS in PM_{2.5} samples.

Table S3. Potential identities and sources for the most intense species from ESI- and ESI+ Mass Spectra (Figure 2).

Table S4. Average values of elemental ratios, molecular weights (MW), double bond equivalents (DBE), modified aromaticity index (AI_{mod}) and carbon oxidation state (OSc) for tentatively identified compounds in ESI- mode of the HULIS samples.

Table S5. Average values of elemental ratios, molecular weights (MW), double bond equivalents (DBEs), modified aromaticity index (AI_{mod}) and carbon oxidation state (OSc) for tentatively identified compounds in ESI+ mode of the HULIS sample.

Table S6. The relative contents of HOA, BBOA, SV-OOA, and LV-OOA groups in HULIS.

Table S7. The relative contents of aliphatic, olefinic, aromatic, and condensed aromatic compounds in HULIS.

Table S8. Correlation coefficient matrix for the meteorological parameters, concentrations of major ion, carbon fraction and optical properties of HULIS in PM_{2.5} samples.

Figure S1. The 24-h air mass backward trajectories at 500 m above ground level before, during, and after the haze episode, determined by the National Oceanic and Atmospheric

Administration Hybrid Single Particle Lagrangian Integrated Trajectory (HYSPLIT) model.

Figure S2. Van Krevelen (VK) diagrams of atomic H/C and N/C ratios for CHN+.

Figure S3. DBE vs. C number for molecular compounds of HULIS from the haze process from ESI- mass spectra.

Figure S4. DBE vs. C number for molecular compounds of HULIS from the haze process from ESI+ mass spectra.

S1. Light absorption

The UV-vis spectra of the WSOC and HULIS samples were measured using a UV–visible spectrophotometer (UV-2600, Shimadzu) and recorded in the range of 200–700 nm with 1 nm intervals. Milli-Q water was used as a blank reference and the spectra were corrected by the filter blanks.

Then the absorption data were converted to the absorption coefficients (Abs_{λ} , unit: Mm^{-1}) and mass absorption efficiency (MAE_{λ} , unit: m^2/gC) following equations S1 and S2 (Li et al., 2019; Wang et al., 2019).

$$Abs_{\lambda} = (A_{\lambda} - A_{700}) \frac{V_l}{V_a \times L} \times \ln(10) \quad (S1)$$

$$MAE_{\lambda} = \frac{Abs_{\lambda}}{C} \quad (S2)$$

where A_{λ} and A_{700} are absorbance at wavelengths λ and 700 nm, respectively. V_l (in mL) corresponds to the volume of water used to extract the filter sample, and V_a (in m^3) is the volume of the air sampled through the filter punch. C is the OC content of WSOC or HULIS in solution (mg/L). Here, $\ln(10)$ is used to convert from the log base-10 to the natural logarithm. MAE_{λ} (m^2/gC) represents mass absorption efficiency of organic matter at wavelength of λ .

The wavelength-dependent light absorption of chromophores in WSOC and HULIS, termed as absorption Ångström exponent (AAE), can be calculated according to the following power law equation (S3) (Li et al., 2019; Yuan et al., 2020):

$$A_{\lambda} = K \cdot \lambda^{-AAE} \quad (S3)$$

where A_{λ} is the absorbance derived from the spectrophotometer at a given wavelength λ (330–400 nm) and K is a constant related to the concentration of chromophores.

S2. FT-ICR MS analysis

A custom software was used to process the mass spectra obtained by FT-ICR MS and the system was operated in both negative (ESI-) and positive (ESI+) modes. In the positive mode, 0–1 of Na is included in the formula calculation because of the high tendency of Na to form adducts with polar organic molecules. The elemental formulas were calculated for each peak in batch mode using custom software, with a signal-to-noise ratio above 10 and a mass tolerance of ± 1 ppm. The identified formulas containing isotopomers (i.e., ^{13}C , ^{18}O , ^{15}N or ^{34}S) are not discussed. Spectra of field blank filters were processed following the same procedure to detect possible contamination.

The double bond equivalent (DBE) provides information on the number of rings plus double bonds in the molecules. The DBE values were obtained based on calculation of the elemental composition $\text{C}_c\text{H}_h\text{O}_o\text{N}_n\text{S}_s$:

$$\text{DBE} = (2c + 2 - h + n)/2 \quad (\text{S4})$$

The modified aromaticity index (AI_{mod}) was calculated based on the following equation proposed by Koch and Dittmar:

$$\text{AI}_{\text{mod}} = (1 + c - 0.5o - s - 0.5h)/(c - 0.5o - s - n) \quad (\text{S5})$$

Here, the AI_{mod} is usually used to classify the nature natural organic matter as aliphatic ($\text{AI} = 0$), olefinic ($0 < \text{AI} < 0.5$), aromatic ($0.5 \leq \text{AI} < 0.67$), and condensed aromatic ($\text{AI} \geq 0.67$) species (Koch and Dittmar, 2006).

Carbon oxidation state (OS_C) was introduced as the degree of oxidation of organic species, which can be obtained according to the following equation (Kroll et al., 2011):

$$\text{OS}_\text{C} \approx 2\text{O}/\text{C} - \text{H}/\text{C} \quad (\text{S6})$$

where O/C and H/C are the elemental ratio of oxygen-to-carbon and hydrogen-to-carbon, respectively.

It is noted that each molecule should present with different intensity, the overall properties of the three HULIS can be calculated with relative abundance weighted. The relative abundance weighted elemental ratios, organic mass to organic carbon ratios, DBE, AI_{mod} and OS_C values are calculated from the intensity (Int) of each assigned peak (*i*) using the following equations (Song et al., 2018):

$$MW_w = \Sigma(MW_i \times \text{Int}_i) / \Sigma \text{Int}_i$$

$$O/C_w = \Sigma(O/C_i \times \text{Int}_i) / \Sigma \text{Int}_i$$

$$H/C_w = \Sigma(H/C_i \times \text{Int}_i) / \Sigma \text{Int}_i$$

$$S/C_w = \Sigma(S/C_i \times \text{Int}_i) / \Sigma \text{Int}_i$$

$$O/N_w = \Sigma(O/N_i \times \text{Int}_i) / \Sigma \text{Int}_i$$

$$O/S_w = \Sigma(O/S_i \times \text{Int}_i) / \Sigma \text{Int}_i$$

$$OM/OC_w = \Sigma(OM/OC_i \times \text{Int}_i) / \Sigma \text{Int}_i$$

$$DBE_w = \Sigma(DBE_i \times \text{Int}_i) / \Sigma \text{Int}_i$$

$$AI_{\text{mod},w} = \Sigma(AI_{\text{mod},i} \times \text{Int}_i) / \Sigma \text{Int}_i$$

$$OS_{C,w} = \Sigma(OS_C \times \text{Int}_i) / \Sigma \text{Int}_i$$

where Int_i is the intensity for each individual molecular formula, *i*.

S3. Chemical analysis

For the water-soluble inorganic species (i.e., Ca^{2+} , Mg^{2+} , K^+ , Na^+ , NH_4^+ , NO_3^- ; SO_4^{2-} , $\text{C}_2\text{O}_4^{2-}$ and Cl^-), a punch ($1.5 \times 1.0 \text{ cm}^2$) of the filters samples were extracted twice with 7 ml ultrapure Milli-Q water for 15 min using an ultrasonic ice-water bath and measured by ion

chromatography (Dionex ICS-900, USA) after filtering through a 0.22 μm pore size PTFE filter. K_{bb}^+ and non-sea salt- SO_4^{2-} were estimated by subtracting the contribution of soil from the total K^+ and SO_4^{2-} (Balasubramanian, 2003). K_{bb}^+ was used to indicate the influence of biomass burning on ambient aerosols (Balasubramanian, 2003).

The levoglucosan was measured and details of chemical isolation and detection methods were similar to the previous study (Wang and Kawamura, 2005). Briefly, the filter-samples were punched and extracted with a DCM/MeOH (2:1, v/v) solution. Then extracts were dehydrated and concentrated to 0.5 mL. 100 μL of extracts were dried by nitrogen and then reacted with derivatization reagents (N, O-bis (trimethylsilyl) trifluoroacetamide (BSTFA) with 1% of trimethylsilyl chloride and pyridine = 5:1, v/v) at 70 $^\circ\text{C}$ for 3 h. Finally, the derivatives were diluted to 0.5 mL and analysed on a gas chromatography-mass spectrometry (Agilent 7890A-5975C, USA) system with a HP-5 MS (30.0 m, 0.25 mm ID, 0.25 mm) capillary column operating under full scan mode.

Table S1. Meteorological parameters and concentrations of carbon fraction and major ion in PM_{2.5} samples.

	Overall (Jan. 7-30)	Clean-I (Jan. 7-12)	Haze-I (Jan. 13-18)	Haze-II (Jan. 19-24)	Clean-II (Jan. 25-30)
PM _{2.5} (μg/m ³)	51 ± 37	18 ± 3.3	82 ± 26	84 ± 22	21 ± 10
WSOC (μgC/m ³)	4.3 ± 1.2	1.2 ± 0.39	8.4 ± 3.4	6.2 ± 1.9	1.3 ± 0.70
HULIS (μgC/m ³)	2.2 ± 1.9	0.46 ± 0.22	4.5 ± 1.2	3.1 ± 1.2	0.75 ± 0.52
EC (μgC/m ³)	1.3 ± 1.2	0.36 ± 0.16	2.7 ± 1.0	1.8 ± 0.58	0.39 ± 0.20
OC (μgC/m ³)	7.6 ± 6.4	2.2 ± 0.85	15 ± 5.4	11 ± 3.0	2.4 ± 1.3
SOC (μgC/m ³)	1.7 ± 1.4	0.64 ± 0.25	3.0 ± 1.4	2.7 ± 0.83	0.66 ± 0.45
OM (μg/m ³)	15 ± 13	4.4 ± 1.7	30 ± 11	22 ± 5.9	4.7 ± 2.6
OC/EC	6.0 ± 0.77	6.4 ± 0.91	5.5 ± 0.47	6.0 ± 0.60	6.0 ± 0.74
WSOC/OC	0.55 ± 0.07	0.55 ± 0.09	0.56 ± 0.03	0.57 ± 0.06	0.53 ± 0.06
HULIS/WSOC	0.50 ± 0.13	0.38 ± 0.09	0.56 ± 0.09	0.49 ± 0.04	0.55 ± 0.17
nss-SO ₄ ²⁻ (μg/m ³)	1.5 ± 0.54	1.4 ± 0.49	1.7 ± 0.41	1.8 ± 0.39	1.2 ± 0.60
NO ₃ ⁻ (μg/m ³)	2.6 ± 1.7	1.4 ± 0.66	4.4 ± 1.4	3.1 ± 1.4	1.4 ± 0.31
NH ₄ ⁺ (μg/m ³)	1.4 ± 1.1	0.47 ± 0.42	2.3 ± 0.91	2.1 ± 1.0	0.54 ± 0.44
Cl ⁻ (μg/m ³)	0.64 ± 0.29	0.42 ± 0.13	0.79 ± 0.35	0.85 ± 0.25	0.51 ± 0.14
Na ⁺ (μg/m ³)	1.2 ± 0.23	1.0 ± 0.20	1.3 ± 0.12	1.3 ± 0.26	1.2 ± 0.21
Mg ²⁺ (μg/m ³)	0.1 ± 0.06	0.07 ± 0.02	0.14 ± 0.08	0.09 ± 0.05	0.09 ± 0.04
Ca ²⁺ (μg/m ³)	0.42 ± 0.07	0.39 ± 0.02	0.48 ± 0.10	0.41 ± 0.06	0.41 ± 0.04
K _{bb} ⁺ (μg/m ³)	0.24 ± 0.19	0.12 ± 0.06	0.33 ± 0.13	0.40 ± 0.22	0.11 ± 0.05
Levoglucosan (ng/m ³)	71 ± 48	33 ± 17	115 ± 43	83 ± 45	61 ± 27
NO ₃ ⁻ /SO ₄ ²⁻	1.4 ± 0.63	0.88 ± 0.43	2.1 ± 0.43	1.4 ± 0.43	1.0 ± 0.43
Others (μg/m ³)	6.6 ± 2.9	7.0 ± 0.64	6.9 ± 0.72	9.1 ± 2.6	3.5 ± 3.0
SO ₂ (μg/m ³)	14 ± 1.6	9.2 ± 1.8	18 ± 2.6	18 ± 3.3	9.7 ± 2.7
NO ₂ (μg/m ³)	77 ± 39	47 ± 6.3	122 ± 32	94 ± 24	46 ± 13
O ₃ (μg/m ³)	66 ± 36	52 ± 30	104 ± 16	69 ± 29	37 ± 26
Relative humidity (%)	66 ± 17	59 ± 28	58 ± 8	71 ± 5	76 ± 5
Temperature (°C)	15 ± 4.5	12 ± 2.3	16 ± 2.8	20 ± 1.6	11 ± 4.5
Wind speed (m/s)	3 ± 1.6	4.1 ± 1.3	1.2 ± 0.25	1.8 ± 70	3.9 ± 1.3

* SOC=OC – (OC/EC)_{pri}×EC, Where (OC/EC)_{pri} is the minimum of OC/EC ratio in each stage; OM=2 × OC. (Chen and Yu, 2007)

Table S2. Average values of Abs₃₆₅, MAE₃₆₅, and AAE of WSOC and HULIS in PM_{2.5} samples.

		Overall	Clean-I	Haze-I	Haze-II	Clean-II
Abs ₃₆₅	WSOC	2.5 ± 2.0	0.76 ± 0.18	4.3 ± 2.0	3.9 ± 1.1	0.89 ± 0.35
	HULIS	1.8 ± 1.6	0.55 ± 0.06	3.4 ± 1.5	2.6 ± 0.85	0.64 ± 0.32
MAE ₃₆₅	WSOC	1.0 ± 0.21	1.1 ± 0.16	0.76 ± 0.05	0.83 ± 0.07	1.1 ± 0.14
	HULIS	1.1 ± 0.27	1.3 ± 0.22	0.91 ± 0.03	0.95 ± 0.11	1.3 ± 0.27
AAE	WSOC	5.2 ± 0.34	4.9 ± 0.55	5.0 ± 0.63	4.4 ± 0.20	4.7 ± 0.33
	HULIS	6.2 ± 0.20	6.2 ± 0.16	6.1 ± 0.09	6.2 ± 0.18	6.1 ± 0.28

Table S3. Potential identities and sources for the most intense species from ESI- and ESI+ Mass Spectra (Figure 2).

Number	Formulas	MASS(Da)	DBE	AI _{mod}	Potential identity	Potential source/precursor	Reference
a	C ₇ H ₇ NO ₃	152.0353	5	0.67	Methylnitrophenol	Biomass burning	(Mohr et al., 2013)
b	C ₈ H ₆ O ₄	165.0193	6	0.67	Phthalic acid	Naphthalene	(Riva et al., 2015)
c	C ₈ H ₉ NO ₃	166.0509	5	0.67	Benzene compound	-	(Lin et al., 2012)
d	C ₈ H ₁₈ O ₄ S	209.0853	0	0.00	Aliphatic organosulfate	Biodiesel and diesel fuel	(Blair et al., 2017)
e	C ₁₀ H ₁₇ NO ₇ S	294.0652	3	0.00	Pinanediol mononitrate	α -pinene; β -pinene; α -terpinene; Terpinolene	(Wang et al., 2019)
f	C ₁₀ H ₁₈ N ₂ O ₁₁ S	373.0559	3	0.00	Pinanediol mononitrate	α -pinene; β -pinene; α -terpinene; Terpinolene	(Wang et al., 2019)
g	C ₁₂ H ₂₃ N	182.1903	2	0.14	Dodecanenitrile	Biomass burning	(Simoneit et al., 2003)

Table S4. Average values of elemental ratios, molecular weights (MW), double bond equivalents (DBE), modified aromaticity index (AI_{mod}) and carbon oxidation state (OSc) for tentatively identified compounds in ESI- mode of the HULIS samples.

Samples	Elemental compositions	Number of formulas	MW_w	H/ C_w	N/ C_w	O/ C_w	S/ C_w	O/ N_w	O/ S_w	OM/ OC_w	DBE_w	DBE/C_w	$AI_{mod,w}$	OSc _w
Clean-I	CHO-	1255	251	1.5	-	0.33	-	-	-	1.6	4.2	0.33	0.21	-0.83
	CHON-	1632	283	1.3	0.10	0.42	-	4.8	-	1.8	6.5	0.50	0.37	-0.42
	CHOS-	478	263	1.9	-	0.58	0.11	-	5.3	2.2	1.8	0.17	0.02	-0.73
	CHONS-	308	308	1.8	0.12	0.91	0.12	7.6	8.1	2.8	2.7	0.29	0.01	0.05
	all in ESI-	3673	266	1.5	0.033	0.45	0.030	1.7	1.6	1.8	4.2	0.34	0.20	-0.65
Haze-I	CHO-	1499	288	1.5	-	0.35	-	-	-	1.6	4.3	0.31	0.18	-0.81
	CHON-	1945	328	1.3	0.09	0.44	-	5.7	-	1.8	6.6	0.46	0.31	-0.44
	CHOS-	576	287	1.9	-	0.56	0.10	-	5.8	2.2	1.9	0.16	0.02	-0.76
	CHONS-	429	333	1.8	0.12	0.90	0.11	8.1	8.6	2.8	2.9	0.28	0.01	0.03
	all in ESI-	4449	302	1.6	0.033	0.47	0.030	2.1	1.9	1.9	4.2	0.32	0.16	-0.63
Haze-II	CHO-	1414	255	1.5	-	0.39	-	-	-	1.6	4.5	0.36	0.21	-0.68
	CHON-	2217	308	1.3	0.10	0.45	-	5.3	-	1.8	6.8	0.49	0.34	-0.38
	CHOS-	696	284	1.9	-	0.59	0.10	-	6.1	2.2	2.0	0.17	0.02	-0.68
	CHONS-	589	333	1.8	0.11	0.86	0.10	8.1	8.5	2.7	3.0	0.28	0.01	-0.04
	all in ESI-	4916	283	1.5	0.036	0.50	0.033	2.2	2.2	1.9	4.3	0.34	0.18	-0.53
Clean-II	CHO-	1091	247	1.5	-	0.34	-	-	-	1.6	4.2	0.34	0.22	-0.80
	CHON-	1379	271	1.2	0.10	0.40	-	4.4	-	1.8	6.6	0.53	0.40	-0.42
	CHOS-	481	276	1.8	-	0.56	0.10	-	5.5	2.2	2.1	0.18	0.02	-0.73
	CHONS-	306	312	1.7	0.11	0.84	0.11	7.7	8.0	2.7	3.0	0.30	0.01	-0.04
	all in ESI-	3257	264	1.5	0.033	0.44	0.029	1.7	1.7	1.8	4.3	0.35	0.21	-0.64

Table S5. Average values of elemental ratios, molecular weights (MW), double bond equivalents (DBEs), modified aromaticity index (AI_{mod}) and carbon oxidation state (OSc) for tentatively identified compounds in ESI+ mode of the HULIS sample.

Samples	Elemental compositions	Number of formulas	MW_w	H/ C_w	N/ C_w	O/ C_w	O/ N_w	OM/ OC_w	DBE $_w$	DBE/ C_w	$AI_{mod,w}$	OSc $_w$
Clean-I	CHO+	1504	236	1.7	-	0.36	-	1.8	2.8	0.22	0.11	-1.0
	CHON+	2213	268	1.6	0.060	0.31	3.5	1.8	4.6	0.33	0.20	-1.0
	CHN+	113	223	1.4	0.10	-	-	1.3	7.4	0.46	0.46	-1.4
	all in ESI+	3830	249	1.7	0.026	0.33	1.4	1.8	3.6	0.27	0.15	-1.0
Haze-I	CHO+	1736	272	1.7	-	0.31	-	1.7	4.0	0.22	0.13	-1.1
	CHON+	2873	317	1.6	0.086	0.27	3.8	1.6	6.6	0.34	0.23	-1.0
	CHN+	165	204	1.6	0.13	-	-	1.3	6.0	0.37	0.37	-1.6
	all in ESI+	4774	290	1.6	0.043	0.28	1.7	1.7	5.3	0.28	0.18	-1.1
Haze-II	CHO+	1794	247	1.7	-	0.34	-	1.7	3.1	0.22	0.12	-1.1
	CHON+	2943	280	1.6	0.094	0.31	3.8	1.7	4.6	0.32	0.19	-1.0
	CHN+	141	209	1.4	0.13	-	-	1.3	6.4	0.44	0.44	-1.4
	all in ESI+	4878	260	1.7	0.042	0.32	1.6	1.7	3.8	0.27	0.15	-1.0
Clean-II	CHO+	1351	241	1.7	-	0.36	-	1.8	3.1	0.23	0.12	-1.0
	CHON+	2008	265	1.6	0.096	0.30	3.4	1.8	4.8	0.34	0.22	-1.0
	CHN+	110	212	1.4	0.14	-	-	1.3	7.2	0.47	0.48	-1.4
	all in ESI+	3469	250	1.7	0.042	0.33	1.4	1.8	3.8	0.28	0.17	-1.0

Table S6. The relative contents of HOA, BBOA, SV-OOA, and LV-OOA groups in HULIS.

Samples	Elemental compositions	ESI- (%)				Elemental compositions	ESI+ (%)			
		HOA	BBOA	SV-OOA	LV-OOA		HOA	BBOA	SV-OOA	LV-OOA
Clean-I	CHO-	4.5	43	24	1.9	CHO+	5.8	72	7.3	0.16
	CHON-	2.3	39	41	6.4	CHON+	13	70	7.7	0.29
	CHOS-	3.0	54	25	2.1	CHN+	8.5	45	0	0
	CHONS-	0	11	54	24	all in ESI+	8.7	71	7.4	0.21
	all in ESI-	3.3	41	31	4.8					
Haze-I	CHO-	18	40	23	1.9	CHO+	10	60	4.4	0.07
	CHON-	8.3	33	36	5.4	CHON+	12	61	4.6	0.14
	CHOS-	5.5	59	25	1.8	CHN+	5.6	34	0	0
	CHONS-	0.49	19	44	24	all in ESI+	11	59	4.3	0.10
	all in ESI-	12	40	29	4.8					
Haze-II	CHO-	3.5	46	28	2.4	CHO+	7.1	72	5.5	0.08
	CHON-	1.2	35	39	6.5	CHON+	11	76	6.7	0.22
	CHOS-	2.8	59	28	2.2	CHN+	4.9	46	0	0
	CHONS-	0.21	20	48	21	all in ESI+	8.8	73	5.9	0.14
	all in ESI-	2.4	43	33	5.4					
Clean-II	CHO-	3.5	43	26	2.1	CHO+	5.0	70	9.7	0.09
	CHON-	1.8	38	43	6.1	CHON+	11	69	7.8	0.22
	CHOS-	3.8	56	26	2.9	CHN+	3.6	51	0	0
	CHONS-	0	13	61	20	all in ESI+	7.5	70	8.8	0.14
	all in ESI-	2.9	42	33	4.6					

Table S7. The relative contents of aliphatic, olefinic, aromatic, and condensed aromatic compounds in HULIS.

Samples	Elemental compositions	ESI- (%)				Elemental compositions	ESI+ (%)			
		Aliphatic	Olefinic	Aromatic	Condensed aromatic		Aliphatic	Olefinic	Aromatic	Condensed aromatic
Clean-I	CHO-	31	53	10	6.0	CHO+	47	50	2.9	0.48
	CHON-	13	54	18	15	CHON+	28	64	6.0	2.0
	CHOS-	86	13	0.56	0	CHN+	4.5	40	33	22.5
	CHONS-	95	4.5	0.22	0.18	all in ESI+	38	56	4.6	1.4
	all in ESI-	42	42	9.6	6.5					
Haze-I	CHO-	29	58	8.1	4.8	CHO+	46	47	4.2	2.6
	CHON-	21	54	15	10	CHON+	29	54	11	6.0
	CHOS-	89	11	0.11	0	CHN+	16	45	21	18
	CHONS-	95	5.0	0.23	0	all in ESI+	37	50	7.7	5.0
	all in ESI-	45	43	7.6	4.7					
Haze-II	CHO-	26	58	10	5.9	CHO+	43	54	2.6	0.52
	CHON-	14	58	16	12	CHON+	29	64	5.2	1.7
	CHOS-	92	7.7	0.19	0.21	CHN+	0.83	51	28	20
	CHONS-	94	6.0	0.19	0.07	all in ESI+	37	58	4.0	1.3
	all in ESI-	45	41	8.4	5.5					
Clean-II	CHO-	31	52	11	6.0	CHO+	45	52	2.9	0.42
	CHON-	8.0	54	22	16	CHON+	25	65	7.3	2.4
	CHOS-	83.5	16	0.52	0	CHN+	5.8	37	33	24
	CHONS-	93	6.8	0.10	0.13	all in ESI+	36	57	5.4	1.6
	all in ESI-	41	42	10	6.7					

Table S8. Correlation coefficient matrix for the meteorological parameters, concentrations of major ion, carbon fraction and optical properties of HULIS in PM_{2.5} samples.

	Abs ₃₆₅	MAE ₃₆₅	AAE	OC	EC	WSOC	HULIS	SO ₂	NO ₂	O ₃	Temp.	Humidity	Levoglucosan	K _{bb} ⁺	NH ₄ ⁺	SO ₄ ²⁻	NO ₃ ⁻	Na ⁺	Cl ⁻	Ca ₂ ⁺	Mg ₂ ⁺	
Abs ₃₆₅	1																					
MAE ₃₆₅	0.696**	1																				
AAE	-0.098	0.156	1																			
OC	0.887**	-0.720**	-0.174	1																		
EC	0.903**	-0.707**	-0.136	0.982**	1																	
WSOC	0.991**	-0.693**	-0.087	0.902**	0.917**	1																
HULIS	0.981**	-0.754**	-0.126	0.922**	0.934**	0.978**	1															
SO ₂	0.864**	-0.828**	-0.120	0.792**	0.819**	0.885**	0.904**	1														
NO ₂	0.947**	-0.729**	-0.073	0.862**	0.860**	0.948**	0.950**	0.890**	1													
O ₃	0.743**	-0.626**	-0.458	0.795**	0.816**	0.760**	0.770**	0.810**	0.781**	1												
Temp.	0.694**	-0.708**	-0.146	0.527*	0.516*	0.701**	0.682**	0.809**	0.769**	0.587*	1											
Humidity	-0.029	0.294	0.336	-0.254	-0.279	-0.042	-0.087	-0.199	-0.073	-0.536*	0.074	1										
Levoglucosan	0.800**	-0.548*	-0.434	0.723**	0.688**	0.797**	0.810**	0.703**	0.787**	0.674**	0.582*	-0.109	1									
K _{bb} ⁺	0.728**	-0.519*	-0.004	0.577*	0.550*	0.711**	0.686**	0.616**	0.648**	0.398	0.622**	0.093	0.742**	1								
NH ₄ ⁺	0.899**	-0.714**	0.085	0.865**	0.840**	0.910**	0.910**	0.816**	0.934**	0.616**	0.717**	0.081	0.731**	0.736**	1							
SO ₄ ²⁻	0.554*	-0.569*	0.291	0.575*	0.515*	0.585*	0.560*	0.489*	0.593*	0.163	0.615**	0.314	0.349	0.523*	0.767**	1						
O ₃ ⁻	0.702**	-0.698**	-0.002	0.860**	0.836**	0.755**	0.789**	0.806**	0.788**	0.706**	0.550*	-0.202	0.567*	0.420	0.837**	0.590*	1					
Na ⁺	0.490*	-0.357	-0.034	0.292	0.300	0.439	0.456	0.342	0.369	0.127	0.294	0.286	0.511*	0.698**	0.470	0.218	0.134	1				
Cl ⁻	0.701**	-0.606**	0.147	0.632**	0.644**	0.708**	0.708**	0.744**	0.852**	0.642**	0.655**	-0.096	0.510*	0.392	0.776**	0.450	0.721**	0.218	1			
Ca ²⁺	0.309	-0.364	-0.273	0.283	0.319	0.247	0.376	0.316	0.256	0.288	0.247	-0.032	0.207	0.145	0.229	0.047	0.165	0.362	0.046	1		
Mg ²⁺	0.309	-0.364	-0.273	0.283	0.319	0.247	0.376	0.316	0.256	0.288	0.247	-0.032	0.207	0.145	0.229	0.047	0.165	0.362	0.046	1	1	

** Correlation is significant at the 0.01 level (2-tailed).

* Correlation is significant at the 0.05 level (2-tailed).

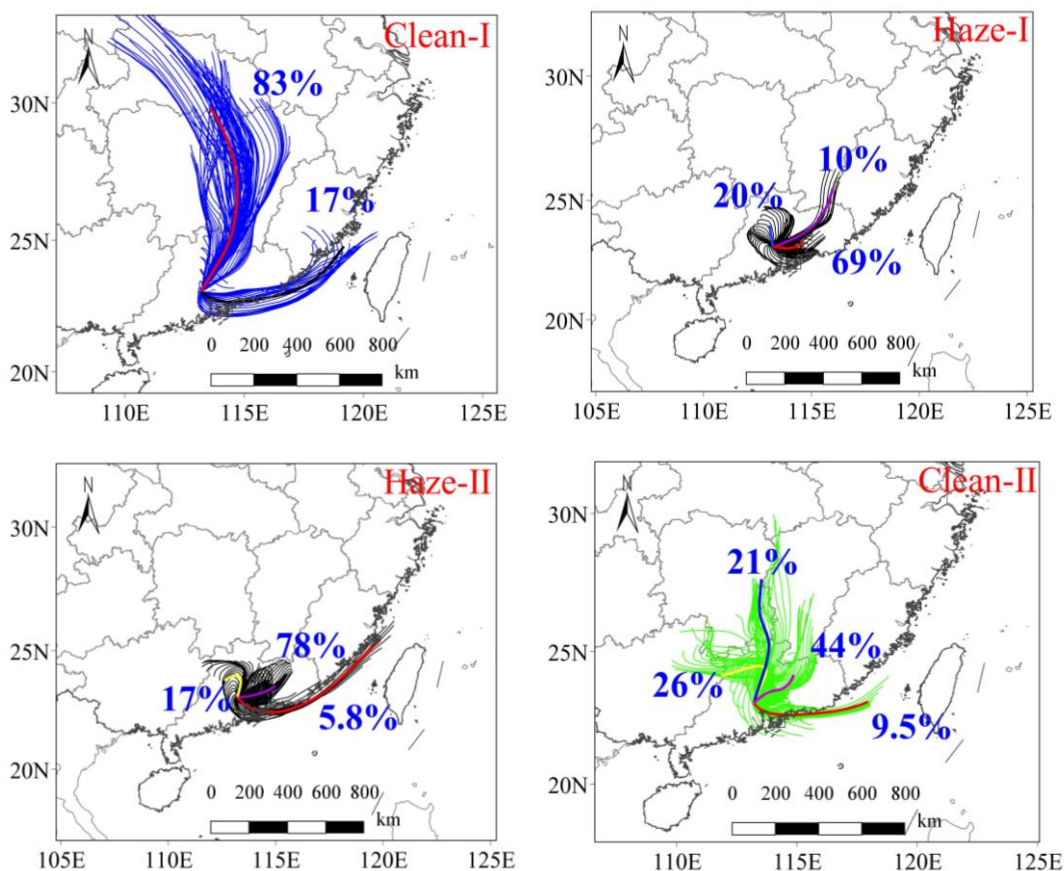


Figure S1. The 24-h air mass backward trajectories at 500 m above ground level before, during, and after the haze episode, determined by the National Oceanic and Atmospheric Administration Hybrid Single Particle Lagrangian Integrated Trajectory (HYSPLIT) model.

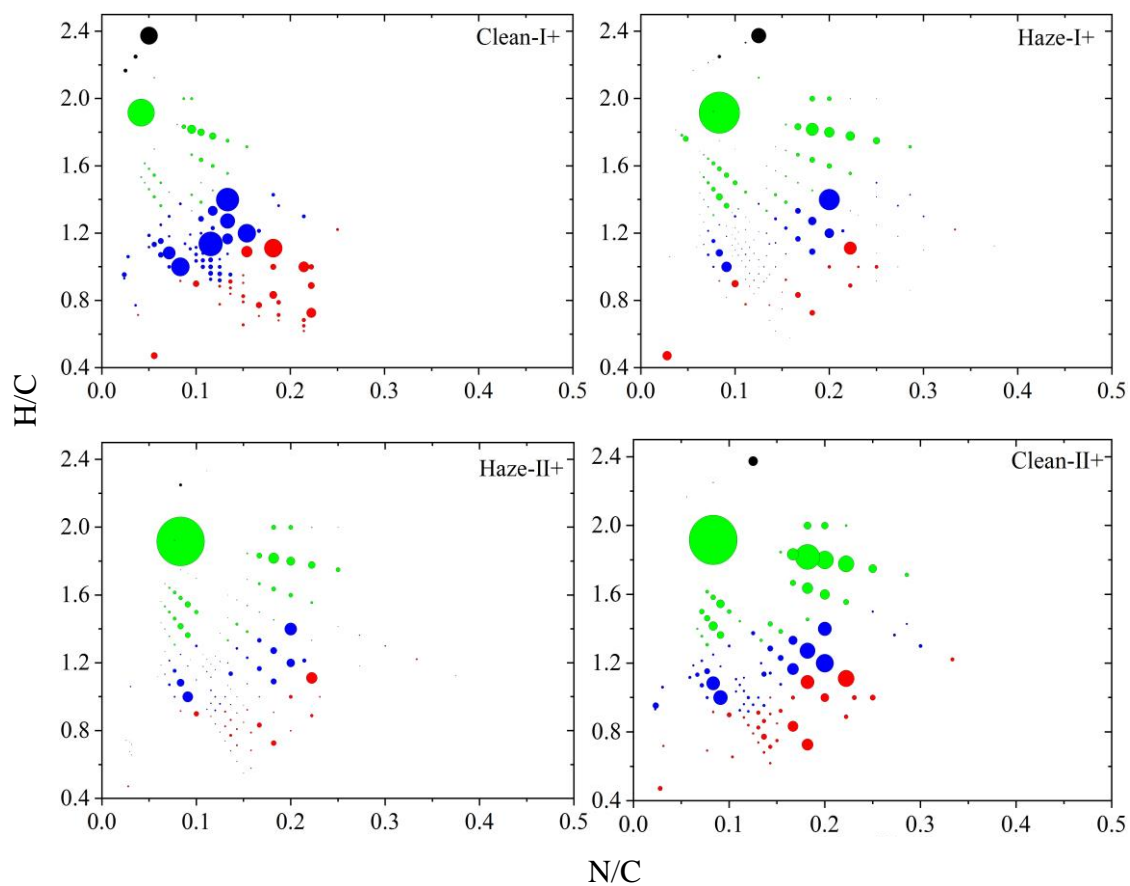


Figure S2. Van Krevelen (VK) diagrams of atomic H/C and N/C ratios for CHN+. Formulas with black, green, blue, and red are assigned to aliphatic (AI = 0), olefinic ($0 < AI < 0.5$), aromatic ($0.5 \leq AI < 0.67$), and condensed aromatic ($AI \geq 0.67$) species (Koch and Dittmar, 2006), respectively.

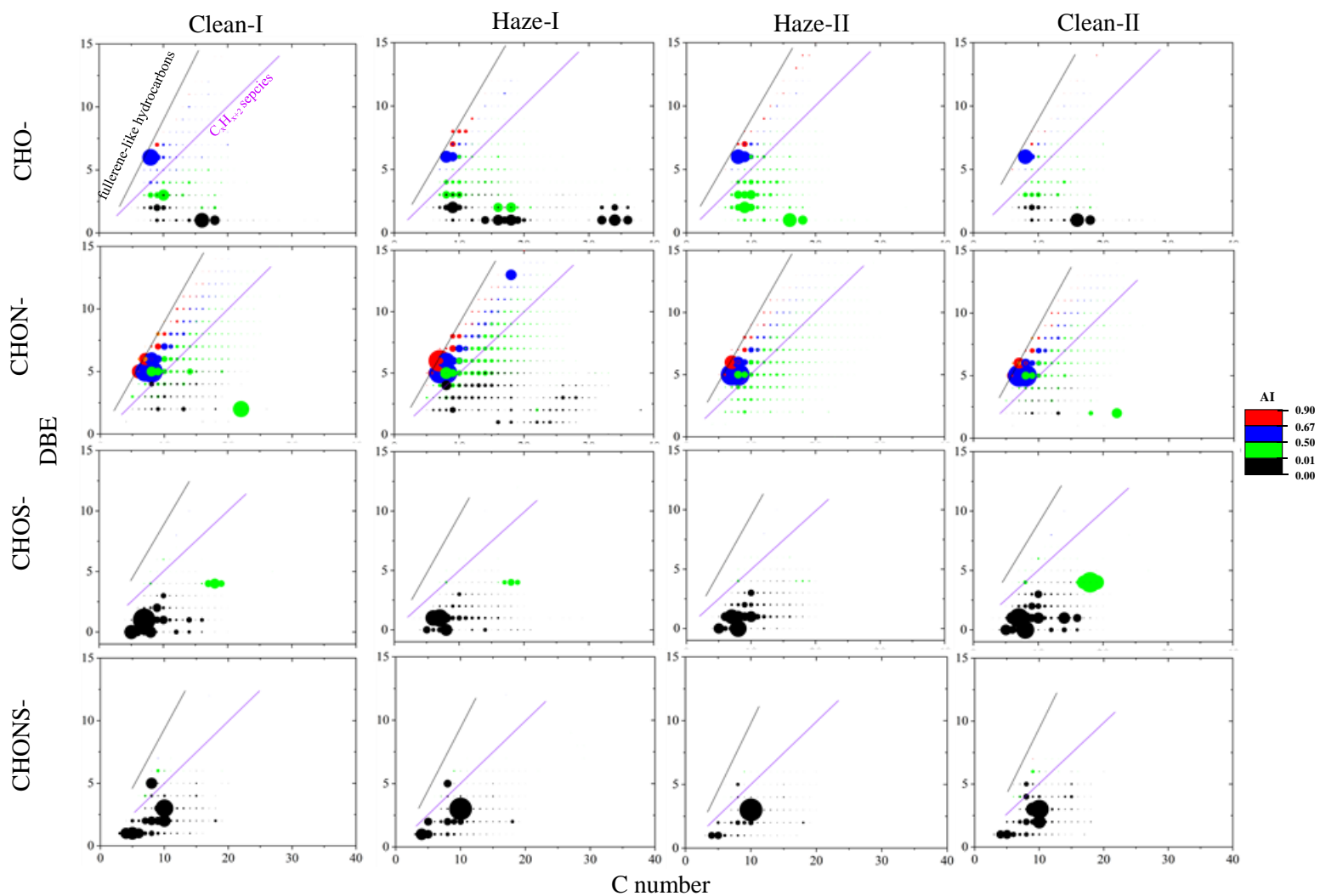


Figure S3. DBE vs. C number for molecular compounds of HULIS from the haze process from ESI- mass spectra. Lines indicate DBE reference values of linear conjugated polyenes C_xH_{x+2} with $DBE = 0.5 \times C$ and fullerene-like hydrocarbons with $DBE = 0.9 \times C$.

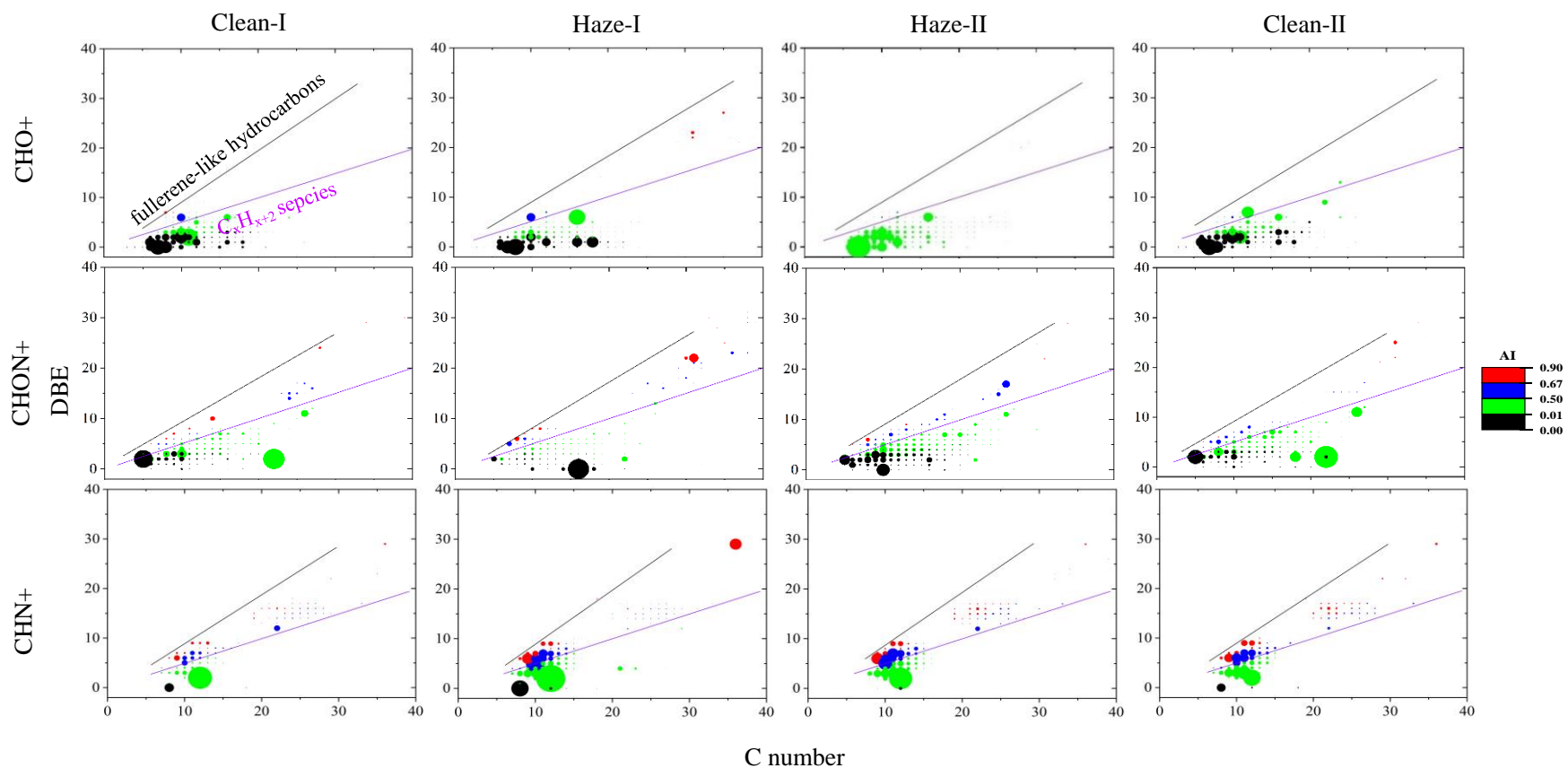


Figure S4. DBE vs. C number for molecular compounds of HULIS from the haze process from ESI+ mass spectra. Lines indicate DBE reference values of linear conjugated polyenes C_xH_{x+2} with $DBE = 0.5 \times C$ and fullerene-like hydrocarbons with $DBE = 0.9 \times C$.

Reference

- Balasubramanian, R.: Comprehensive characterization of PM_{2.5} aerosols in Singapore, *Journal of Geophysical Research*, 108, 10.1029/2002jd002517, 2003.
- Koch, B. P. and Dittmar, T.: From mass to structure: an aromaticity index for high-resolution mass data of natural organic matter, *Rapid Commun Mass Sp*, 20, 926-932, 10.1002/rcm.2386, 2006.
- Kroll, J. H., Donahue, N. M., Jimenez, J. L., Kessler, S. H., Canagaratna, M. R., Wilson, K. R., Altieri, K. E., Mazzoleni, L. R., Wozniak, A. S., Bluhm, H., Mysak, E. R., Smith, J. D., Kolb, C. E., and Worsnop, D. R.: Carbon oxidation state as a metric for describing the chemistry of atmospheric organic aerosol, *Nature Chemistry*, 3, 133-139, 10.1038/nchem.948, 2011.
- Li, M., Fan, X., Zhu, M., Zou, C., Song, J., Wei, S., Jia, W., and Peng, P.: Abundance and light absorption properties of brown carbon emitted from residential coal combustion in China, *Environ Sci Technol*, 53, 595-603, 10.1021/acs.est.8b05630, 2019.
- Song, J., Li, M., Jiang, B., Wei, S., Fan, X., and Peng, P.: Molecular characterization of water-soluble humic like substances in smoke particles emitted from combustion of biomass materials and coal using Ultrahigh-resolution electrospray ionization fourier transform ion cyclotron resonance mass spectrometry, *Environ Sci Technol*, 52, 2575-2585, 10.1021/acs.est.7b06126, 2018.
- Wang G , K. K.: Molecular Characteristics of Urban Organic Aerosols from Nanjing- A Case Study of A Mega-City in China, *Environmental ence & Technology*, 18, 2005.
- Wang, Y., Hu, M., Lin, P., Tan, T., Li, M., Xu, N., Zheng, J., Du, Z., Qin, Y., Wu, Y., Lu, S., Song, Y., Wu, Z., Guo, S., Zeng, L., Huang, X., and He, L.: Enhancement in Particulate Organic Nitrogen and Light Absorption of Humic-Like Substances over Tibetan Plateau Due to Long-Range Transported Biomass Burning Emissions, *Environ Sci Technol*, 53, 14222-14232, 10.1021/acs.est.9b06152, 2019.
- Yuan, W., Huang, R.-J., Yang, L., Guo, J., Chen, Z., Duan, J., Wang, T., Ni, H., Han, Y., Li, Y., Chen, Q., Chen, Y., Hoffmann, T., and O'Dowd, C.: Characterization of the light-absorbing properties, chromophore composition and sources of brown carbon aerosol in Xi'an, northwestern China, *Atmospheric Chemistry and Physics*, 20, 5129-5144, 10.5194/acp-20-5129-2020, 2020.